ACS APPLIED MATERIALS & INTERFACES

Research Article

www.acsami.org

Modification of TiO_2 Electrode with Organic Silane Interposed Layer for High-Performance of Dye-Sensitized Solar Cells

Galhenage A. Sewvandi, Zhuoqi Tao, Takafumi Kusunose, Yasuhiro Tanaka, Shunsuke Nakanishi, and Qi Feng*

Department of Advanced Materials Science, Faculty of Engineering, Kagawa University, 2217-20 Hayashi-cho, Takamatsu 761-0396, Japan

Supporting Information

ABSTRACT: Back electron transfer from the TiO_2 electrode surface to the electrolyte is the main reason behind the low-open circuit potential (V_{oc}) and the low-fill factor (FF) of the dye-sensitized solar cells (DSSCs). Modifications to the TiO_2 electrode, fabricated using {010}-faceted TiO_2 nanoparticles with six different kinds of silane, are reported to decrease the back electron transfer on the TiO_2 surface. The effect of alkyl chain length of hydrocarbon silanes and fluorocarbon silanes on adsorption parameters of surface coverage and adsorption constant, interfacial resistance, and photovoltaic performances were investigated. Adsorption isotherms, impedance analysis, and photovoltaic measurements were used as the investigation techniques. The reduction of back electron transfer depended on the TiO_2 surface coverage by silane, alkyl chain length, and the molecular structure of the silane. Even though V_{oc} and FF were improved, significant reduction in short-circuit photocurrent density (J_{sc}) was observed after silanization because of desorption of dye during silanization. A new approach, sequential adsorption process of silane and dye, was introduced to enhance V_{oc} and FF without lowering J_{sc}. Heptadecafluorodecyl trimethoxy-silane showed the highest coverage on the surface of the TiO_2 and had the highest effect on the performance improvement of the DSSC, where V_{oc}, FF, and efficiency (η) were improved by 22, 8.0, and 22%, respectively.

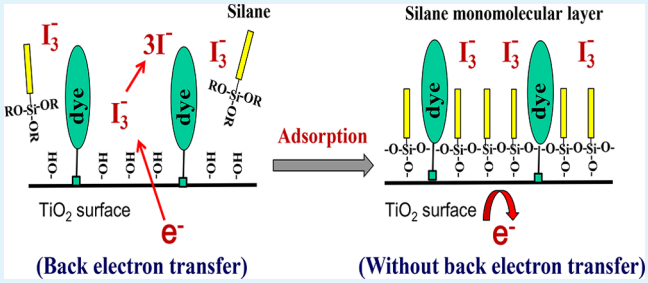

KEYWORDS: *dye-sensitized solar cells, adsorption isotherms, silanization, back electron transfer, photovoltaic performances, sequential adsorption*

1. INTRODUCTION

Dye-sensitized solar cells (DSSCs) have attracted great interest from scientists because they have the potential to convert sunlight (solar power) to electricity (electrical power) at a low cost in an environmentally friendly way.[1] A typical DSSC consists of a dye-sensitized TiO_2 electrode, a Pt electrode, and an electrolyte. Figure 1 shows the working principle of the DSSC; namely, (1) excitation process, (2) injection process, (3) energy generation, (4) regeneration of the mediator, and (5) regeneration of dye.[2] However, as shown in Figure 1, it is possible for backward reactions to occur, which would yield a substantially diminished return. The possible backward reactions are (6) the excited electron in LUMO (lowest unoccupied molecular orbital) level of the dye can be recombined with the hole in its HOMO (highest occupied molecular orbital) level, (7) the injected electrons in the TiO_2 conduction band can be recombined with I_3^- ions in the electrolyte, (8) the electrons in the TiO_2 conduction band can be recombined with holes in the HOMO level of the dye, and (9) the electrons in the conducting glass can be recombined with I_3^- ions in the electrolyte.[3]

These backward reactions will result in decreased efficiencies of DSSCs. But dye regeneration reaction (5) and electron injection from the LUMO level of the dye to the conduction band of TiO_2 (2) are taken at fast rates (ns and ps).[4] The length of time takes for an electron to diffuse through TiO_2 nanoparticles to the conducting glass surface is about 10 ms.[3,4] This provides ample time for the back electron transfer from TiO_2 surface to oxidized redox species in the electrolyte. Therefore, a major limitation of DSSCs efficiencies is the loss of injected electrons from the semiconductor to the oxidized redox species in the electrolyte. That means the reaction shown by arrow (7) in Figure 1 is the prominent backward reaction that should be eliminated to get high efficiency. Our recent study on dye adsorption on TiO_2 electrode surfaces has suggested that only about one-third of the TiO_2 electrode surface is covered by the adsorbed-dye molecules and two-thirds of the surface is exposed to the electrolyte solution.[5] The uncovered area is potential site for interfacial back electron transfer which is represented by arrow (7). Thus, it is necessary to reduce the rate of the backward reaction at the TiO_2 surfaces in DSSCs.

Received: January 30, 2014
Accepted: March 31, 2014
Published: March 31, 2014

   dx.doi.org/10.1021/am500666e | ACS Appl. Mater. Interfaces 2014, 6, 5818−5826

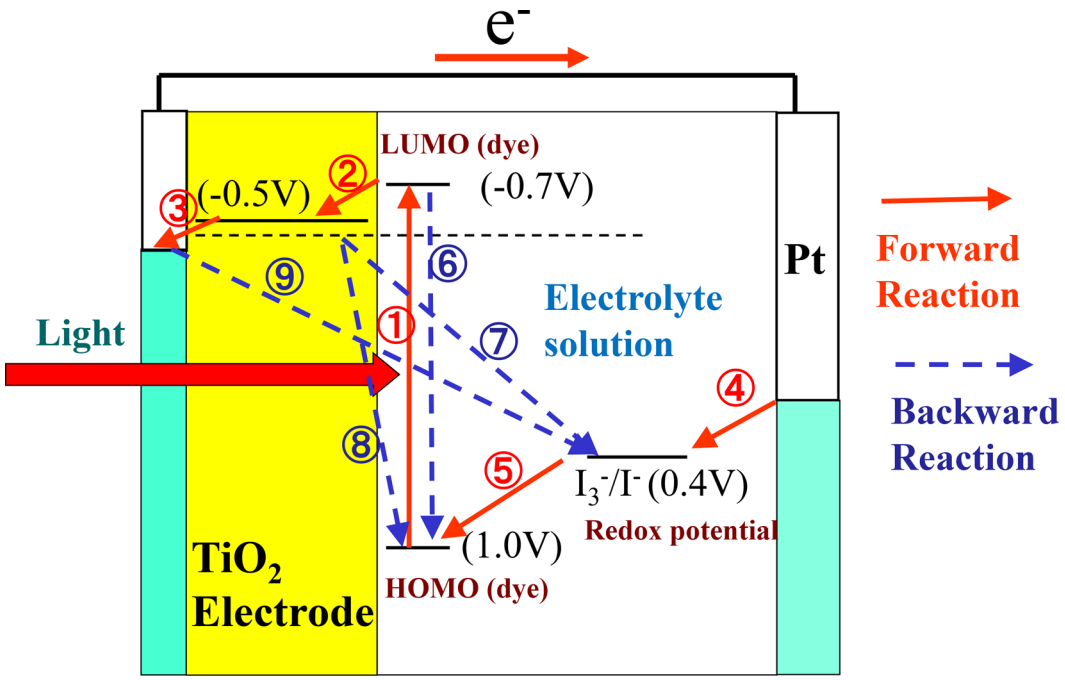

Figure 1. Working principle of a typical dye-sensitized solar cell.

Extensive studies on minimizing the back electron transfer have been reported. The addition of additives to redox electrolyte, such as 4-*tert*-butylpyridine (TBP) and guanidinium thiocyanate (GuSCN), have suppressed the back electron transfer by adsorbing these additives on the surface of the TiO_2 electrode.[6−9] Because these cations formed weak bonds on the TiO_2 surface, stronger surface modification technique should be investigated. The TiO_2 under layer on conducting glass substrate (FTO) has reduced the back electron transfer on the FTO surface.[10,11] But the back electron transfer on the TiO_2 surface is much higher than that on the FTO surface because of the large surface area of TiO_2, that is two-thirds of its surface, is exposed to the electrolyte solution.[5] Limited studies have been reported in TiO_2 surface passivation using silanes.[3,12−14] The silane adsorption process is a chemisorption process. Therefore, it can cover the exposed TiO_2 surface with a covalently bonded strong silane monomolecular layer to decrease the rate of the back electron transfer by physically preventing the close approach of I_3^- to the TiO_2 electron surface.

A couple of studies have reported on the dye-sensitized TiO_2 surface passivation,[3,12] using CH_3SiCl_3 as a silanization agent with the kinetically fast redox couples. Another couple of approaches have been reported to reduce the back reaction using alkyl(trialkoxy)silanes with iodine redox couple, and it suggested that the DSSCs performance depends on the length of the alkyl chain of the silane and the composition of the electrolyte.[13,14] Nevertheless, although silane adsorption is an effective way to enhance DSSC performance, to the best of our knowledge, it has not been reported so far on the effects of silanes adsorption parameters of silane coverage and adsorption constant, concentration, and the treatment sequences of silanes on the photovoltaic performances.

In this study, we describe the effects of alkyl-chain length and substitution of the silane coupling agent on the adsorption parameters of adsorption density and adsorption constant, interfacial resistance, electron lifetime, and photovoltaic performances of DSSCs. We focus on the modification of the exposed TiO_2 surface because in our previous study, we found that anatase cubic {010}-faceted TiO_2 nanoparticles show a specific high short-circuit current density (J_{sc} = 21 mA/cm^2), but low open-circuit voltage (V_{oc}) and fill factor (FF) as a result of the low dye coverage (33%) on the TiO_2 surface, which leads a large back electron transfer.[5] It suggests that a high-performance DSSC can be obtained using {010}-faceted TiO_2 nanoparticles by blocking the back electron transfer. In-depth studies on silanization processes are carried out to minimize the dye desorption during silanization and to optimize the DSSC performance by optimizing the silanization process.

2. EXPERIMENTAL SECTION

2.1. Chemicals and Reagents. N719 (cis-di (thiocyanate)bis-(2,2′-bipyridyl-4,4′-dicarboxylate)-ruthium(II) (bis-tetrabutylammonium) purchased from Sigma-Aldrich, was used as the dye sensitizer. Other chemicals and reagents were analytical grade and used as received. Six kinds of siloxanes with different end groups as given in Table 1 were used in the present study. These siloxanes were purchased from Shin-Etsu Chemicals.

2.2. Silane Adsorption on TiO_2 Nanoparticles. A 50 mg portion of TiO_2 nanoparticles were added to 10 mL of the solution of

Table 1. Surface Modifying Organic Silane Agents Used in This Study

chemical name	chemical formula	abbreviation
trimethoxy(3,3,3-trifluoropropyl)-silane	$CF_3C_2H_4Si(OCH_3)_3$	FOS-C3F3
hexyltrimethoxy-silane	$C_6H_{13}Si(OCH_3)_3$	HOS-C6
decyltrimethoxy-silane	$C_{10}H_{21}Si(OCH_3)_3$	HOS-C10
octadecyltrimethoxy-silane	$C_{18}H_{37}Si(OCH_3)_3$	HOS-C18
heptadecafluorodecyl trimethoxy-silane	$C_{10}F_{17}H_4Si(OCH_3)_3$	FOS-C10F17
N-[3-(trimethosysilyl)propyl] aniline-silane	$C_6H_5N(CH_2)_3Si(OCH_3)_3$	KMB

dx.doi.org/10.1021/am500666e | ACS Appl. Mater. Interfaces 2014, 6, 5818−5826

silane in ethanol and the silane concentration was maintained within a range of 0.01−0.3 mol/L. Then, it was allowed to adsorb at room temperature for the desired length of time. After that, the solution was centrifuged at a rate of 4000 rpm for 10 min and the supernatant was removed. Solid phase was washed in ethanol to remove physically adsorbed silanes. Then, it was dried at 60 °C for 24 h followed by TG-DTA analysis. The adsorbed amount of silane was measured using weight loss in a temperature range of 200−500 °C in TG-DTA curves, (see Figure S1 in the Supporting Information) which correspond to the decomposition of silane.[15]

2.3. Fabrication of TiO_2 Electrode. Anatase {010}-faceted TiO_2 nanoparticles with cubic morphology, particle size of about 20 nm, and BET surface area of 131 m^2/g, were used in the fabrication of TiO_2 electrode. The TiO_2 nanoparticles were synthesized using the hydrothermal soft chemical method from layered titanate nanosheets.[16] The TiO_2 paste and the TiO_2 electrode were prepared as described in our previous study.[5] The thickness of the TiO_2 porous film was controlled in a rage of 8−13 μm. For the fabrication of an optimized TiO_2 electrode, leaflike anatase particles[16] with a size of 150 nm in length and 30 nm in width were used in the scattering layer.

2.4. Dye and Silane Adsorptions on TiO_2 Electrode. A 0.3 mmol/L N719 dye solution was used for dye adsorption. The dye loaded TiO_2 electrode was immersed in solution of silane in ethanol for 2 h. The electrode was then rinsed copiously in ethanol and allowed to dry at room temperature.

2.5. Fabrication of DSSC. The DSSC was composed of the dye-adsorbed TiO_2 electrode and a Pt-coated FTO conducting glass counter-electrode, with an electrolyte solution between the electrodes. Two types of electrolytes were employed in this work: (1) 0.6 M LiI and 0.03 M I_2 in a mixed solvent of acetonitrile and valeronitrile (85%:15% volume ratio); (2) 0.6 M butylmethylimidazolium iodide, 0.01 M I_2, 0.1 M LiI, 0.1 M guanidinium thiocyanate, and 0.4 M 4-tert-butylpyridine in a mixed solvent of acetonitrile and valeronitrile (85%:15% volume ratio).

2.6. Characterization. Fourier transform infrared (FT-IR) spectra were obtained using a PerkinElmer Spectrum One spectrometer at a resolution of 2 cm^{-1} using the KBr technique in the range of 300 to 4000 cm^{-1}. The photocurrent−voltage (I−V) curves were obtained using a Hokuto-Denko BAS100B electrochemical analyzer with a YSS-E40 Yamashita Denso solar simulator (AM 1.5; 100 mW/cm^2). Electrochemical impedance measurements were performed with an impedance analyzer (Solartron SI 1287) under dark condition. The impedance spectra were recorded in a frequency range of 0.1 Hz to 1 MHz with alternate current (AC) amplitude of 10 mV at an applied direct current (DC) bias of −0.7 V. Thermogravimetric and differential thermal analyses (TG-DTA) were carried out using a Shimadzu DTG-60H at a heating rate of 10 °C/min.

3. RESULTS AND DISCUSSION

3.1. Adsorption of Organic Silanes on TiO_2 Nanoparticles. The IR spectra of TiO_2 powder samples after the FOS-C3F3 silane adsorption treatment at different time intervals are shown in Figure 2. In the IR spectra, absorption bands at 2850 and 2950 cm^{-1} can be assigned to the asymmetric and symmetric stretching of CH_2 groups on the alkyl chain, absorption band at 1404 cm^{-1} to the stretching of C−F bond, and absorption band at 1050 cm^{-1} to stretching of Si−O, respectively.[14,17−19] The intensity ratios of the silane (Si−O) vibration band to Ti−O vibration band of TiO_2 at 700 cm^{-1} increased with increasing the adsorption treatment time up to 2 h, and then became almost constant (see Figure S2 in the Supporting Information). These results reveal that FOS-C3F3 silane molecules are adsorbed on the TiO_2 particle surface, and the silane adsorption almost reaches equilibrium after 2 h. Therefore, a silanizing treatment time of 2 h was used in the next steps.

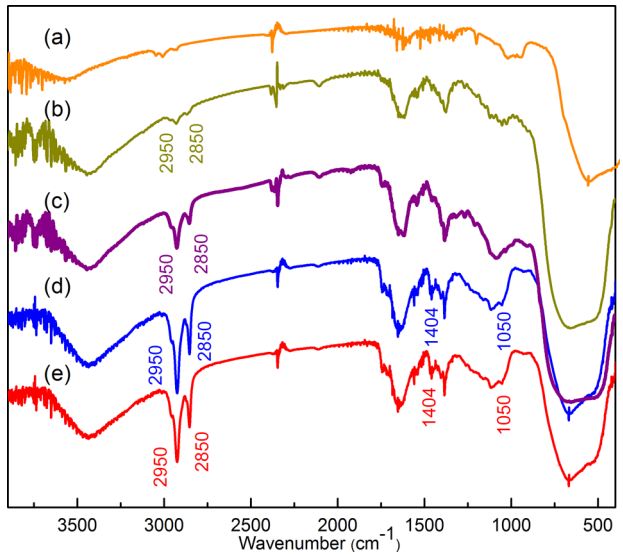

Figure 2. IR spectra of TiO_2 electrodes silanized with FOS-C3F3 for (a) 0, (b) 0.5, (c) 1, (d) 2, and (e)5 h.

To investigate the effect of silane concentration, alkyl chain length, and substitutes on the self-assembled monolayers (SAMs) formation, adsorption isotherm studies were performed with six different modifiers (Table 1) with the TiO_2 nanoparticles at room temperature. Adsorption isotherm results are shown in Figure 3. To more clearly understand the situation of the silane molecules adsorbed on the TiO_2 nanoparticle surface, we present the silane adsorption amount as per BET specific surface area (S_{BET}) of the powder sample that corresponds to silane adsorption density on the nanoparticle surface (mol/m^2). The experimental data of the silanes adsorption were compliant with the Langmuir isotherm, indicating Langmuir monolayer adsorption, meaning typical chemisorption, on the TiO_2 nanocrystals.[5,6,20]

The Langmuir equation can be represented by the following linear formula:

$$C/Q = 1/(Q_m K_{ad}) + C/Q_m \quad (1)$$

where C, Q, Q_m, and K_{ad} are the equilibrium concentration of the silane solution, adsorption density at concentration C, saturation or maximum adsorption density, and adsorption constant, respectively. The least-squares values (R^2) of the experiment results fitting to formula 1 are 0.997 for HOS-C3F3, 0.997 for HOS-C6, 0.997 for HOS-C10, 0.999 for HOS-C18, 0.999 for FOS-C10F17, and 0.999 for KMB. The adsorption constant and maximum adsorption density can be calculated by plotting C/Q against C, and the results are tabulated in Table 2. The silanes adsorption densities ($Q_{0.06}$) at 0.06 M silane concentration are also given in Table 2 because this concentration of silane solutions is used in the TiO_2 electrode modification. The TiO_2 surface coverage by adsorbed silane molecules can be calculated using following formula:

$$S = QN_A A \cdot 100\% \quad (2)$$

where S (%), Q (mol/m^2), N_A (6.022×10^{23} mol^{-1}), and A (m^2) are surface coverage, adsorption density, Avogadro constant, and cross-sectional area of the silane molecule, respectively. Maximum coverage and coverage at 0.06 M silane concentrations are shown in Table 2.

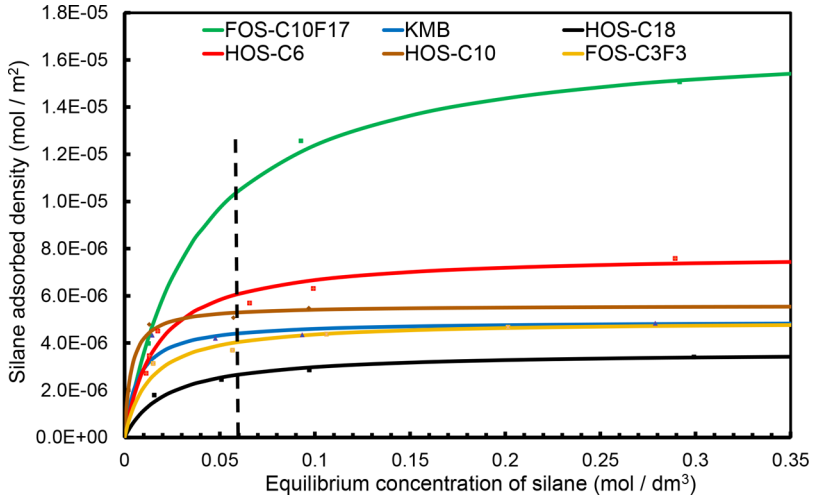

Figure 3. Adsorption isotherms of HOS-C6, HOS-C10, HOS-C18, FOS-C3F3, FOS-C10F17, and KMB silanes on TiO_2 nanoparticles.

Table 2. Silane Adsorption Parameters on TiO_2 Nanoparticles and the Interfacial Resistance of TiO_2 Electrode without Dyeing

silane modifier	Q_m (mol/m^2)	K_{ad} (dm^3/mol)	$Q_{0.06}$ (mol/m^2)	maximum surface coverage(%)	surface coverage at 0.06 mol/dm^3(%)	R_{rc} (Ω)
nonmodified						150
FOS-C3F3	4.9×10^{-6}	7.5×10^{4}	4.0×10^{-6}	24	20	215
HOS-C6	7.6×10^{-6}	16×10^{4}	6.1×10^{-6}	38	30	310
HOS-C10	5.5×10^{-6}	13×10^{4}	5.3×10^{-6}	27	26	200
HOS-C18	3.5×10^{-6}	4.6×10^{4}	2.7×10^{-6}	17	13	700
FOS-C10F17	17×10^{-6}	2.6×10^{4}	10×10^{-6}	85	50	1400
KMB	4.9×10^{-6}	14.2×10^{4}	4.4×10^{-6}	24	22	60

K_{ad}, Q_m, $Q_{0.06}$, and surface coverage for SAMs of hydrocarbon silane decrease with increasing alkyl chain length (HOS-C6 > HOS-C10 > HOS-C18). Because, as the length of alkyl chain is increased, the interchain interactions become dominated by alkyl−alkyl interaction which leads to increase steric hindrance between silane molecules, namely, compared to long-chained silane, short-chained silane could allow more silane molecules to approach the exposed surface. FOS-C3F3 and FOS-C10F17 behave in different ways compared with hydrocarbon silanes. Surface coverage, Q_m, and $Q_{0.06}$ increased with increasing fluorocarbon chain length and K_{ad} decreased. The highest maximum surface coverage of 85% is given with FOS-C10F17. The surface of closely packed fluorocarbon groups has the lowest possible surface energy.[21] The low polarizability and high-ionization potential of the C−F bond due to electronegativity of fluorine show weak intermolecular attractive forces compared with hydrocarbon. It results in closely packed SAM with FOS-C10F17. We think that the silane adsorption would also be affected by TiO_2 nanoparticle surface properties, and the different facets on TiO_2 nanocrystals would show different silane adsorption abilities; due to their different surface energies and different Ti−OH densities on the surfaces.

Electrochemical impedance spectroscopy (EIS) is a powerful, versatile technique to study the electron transfer and the back electron transfer in DSSC system.[22,23] EIS was performed to investigate the effect of silanization on the back electron transfer process. The back electron transfer resistance (R_{rc}) on TiO_2/electrolyte interface (interfacial resistance) was estimated using Nyquist plot (see Figure S3 in the Supporting Information.) obtained from electrochemical impedance spectroscopy and a DSSC equivalent circuit as shown in Figure S4 in the Supporting Information.

The results are summarized in Table 2. With the exception of KMB, the value of R_{rc} increase after silanization, suggesting that they have a potential to reduce the back electron transfer. Among the DSSC cells modified with hydrocarbon silanes, HOS-C6, HOS-C10, and HOS-C18, HOS-C18 which has the longest alkyl chain shows the lowest coverage and the largest R_{rc} value. The results suggest that the R_{rc} value is dependent, not only on the coverage on TiO_2 surface, but also on the alkyl-chain length. FOS-C10F17 shows the highest interfacial resistance, whereas KMB is the lowest. It is possible for unsaturated benzene group in KMB to be worked in a favorable way to electron-recombination process. Therefore, further investigation was carried out using hydrocarbon and fluorocarbon silanes.

3.2. Adsorption of Organic Silane on Dye-Sensitized TiO_2 Electrodes. HOS-C6 silane was used in the studies of silane adsorption on a dye-sensitized TiO_2 electrode in detail. The dye-sensitized TiO_2 electrode was treated in various concentrations of HOS-C6 solutions. The amount of silane and the amount of dye adsorbed by TiO_2 electrode were calculated using weight loss corresponding to decomposition of HOS-C6 in the temperature range of 200 to 350 °C and dye in the temperature range of 350 to 450 °C in TG-DTA curves, respectively (see Figure S5 in the Supporting Information). The results (Figure 4) illustrate that with increasing the silane concentration from 0 to 0.1 M, the amount of silane uptake increases greatly and the amount of dye uptake decreases slightly, afterward both of them become nearly constant. The results suggest that silanization causes partial dye desorption from the TiO_2 surface.

The DSSCs were fabricated using dyed/silanized TiO_2 electrodes and $I-V$ performances were measured. To understand the silane modification effect on the DSSC performance,

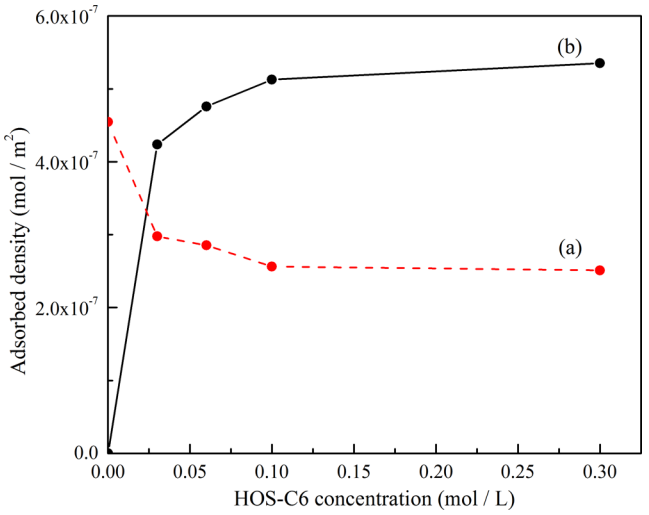

Figure 4. Adsorbed densities of (a) N719 dye and (b) silane at different HOS-C6 concentrations.

0.1 M LiI and 1.0 M I_2 in a mixed solvent of acetonitrile and valeronitrile (85%:15% volume ratio) was used as the electrolyte without any additives. The obtained results are shown in Figure 5. As shown in Figure 5a, open-circuit photovoltage (V_{oc}) has increased from 0.38 to 0.48 V while increasing HOS-C6 concentration 0 to 0.06 M and then it has become constant. On the other hand, the current density (J_{sc}) is reduced from 16 mA/cm^2 to 10 mA/cm^2. When the silane concentration is increased, the fill factor (FF) also increases from 31% without silanization to 60% at 0.1 M silane and then continues to decrease slightly. Efficiency (η) has also followed the similar pattern to the FF (Figure 5b). The improvements in V_{oc} and FF can be attributed to increase in the amount of silane adsorbed on the TiO_2 surface which insulates the surface from the electrolyte solution as shown in Figure 6. The silane molecules and dye molecules adsorbed on the TiO_2 surface block the back electron transfer from the TiO_2 surface to I_3^- in the electrolyte solution. We think that one reason for the little decrease in FF at high silane concentration may be attributed to the dye desorption because the adsorbed dye molecules can also block the back electron transfer similar to silane. Under the high silane concentration conditions, the adsorption of silane molecules on the dye-uncovered area has reached almost saturation, and then further adsorption of silane will accompany desorption of dye. The maximum coverage by both of silane and dye maybe reach at around 0.1 mol/dm^3 where shows the largest FF value. It has been reported that the FF is also affected by other factors,[23] these factors maybe affect the FF value. For example, a physical adsorption of silane onto the dye molecules could inhibit the dye regeneration reaction,[12] which will also reduce the FF value. The silane adsorption onto the dye molecules would increase with increasing the silane concentration.

At 0.06 M silane concentration, 37% of dye is desorbed and J_{sc} is reduced by 36%. It suggests that the main reason for the reduction of J_{sc} is the dye desorption during silanization. This result is also consistent with that the silane adsorption does not adversely affect electron injection yields from dye to TiO_2.[14] Therefore, to get optimum performance, the silane should form bonds only on the uncovered area of the TiO_2 electrode without damaging or removing the dye as demonstrated in Figure 6. The back electron transfer under illumination was qualitatively examined by dark-current density. As shown in dark $I-V$ curves (Figure 7), the presence of silane had a significant effect on dark-current density. Dark-current density has reduced significantly after silanization. This is consistent with the dependency of V_{oc} and FF on HOS-C6 concentration.

From these results, it was identified that dye adsorption and silane adsorption should be controlled to get high performance. In other words, silane concentration is one of the critical parameters to obtain optimum performance. It should be maintained the silane concentration to make larger surface coverage without damaging or removing dye molecules. In this study, maximum V_{oc} as well as relatively high FF and η were observed around 0.06 M HOS-C6 concentrations. Therefore, 0.06 M was selected for the next steps.

3.3. Effect of Silanization-Process Sequence. Although V_{oc}, FF, and η were improved by silanization, J_{sc} was decreased as a result of desorption of adsorbed dye after silanization. In this section, our approach is focused to improve J_{sc} by changing the TiO_2 electrode treatment sequence of dye and silane. The sequential adsorption of dye has been the focus of many investigations. In this process, adsorption of adsorbate can be controlled by simply changing adsorption time, concentration, and sequence of adsorption. Sequential adsorption of different type of dyes[24−26] and sequential adsorption of dyes and coadsorbent[27] in DSSC fabrication have been reported.

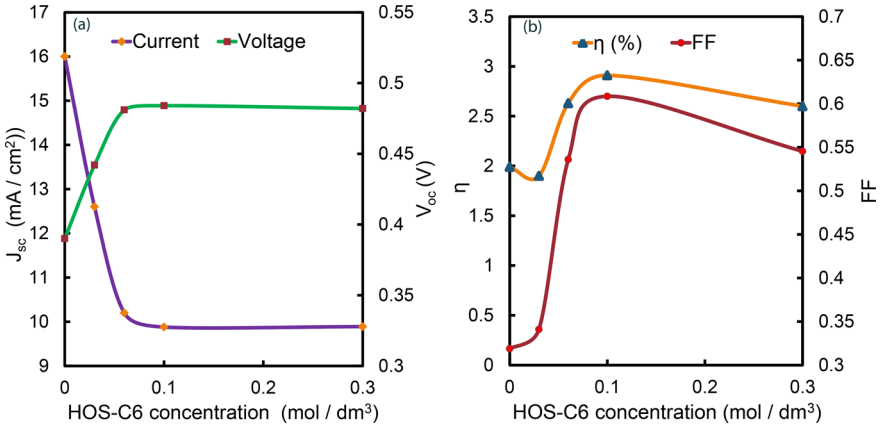

Figure 5. Dependences of DSSCs cell parameters on HOS-C6 concentration: (a) current density (J_{sc}) and voltage (V_{oc}); (b) fill factor (FF) and efficiency (η).

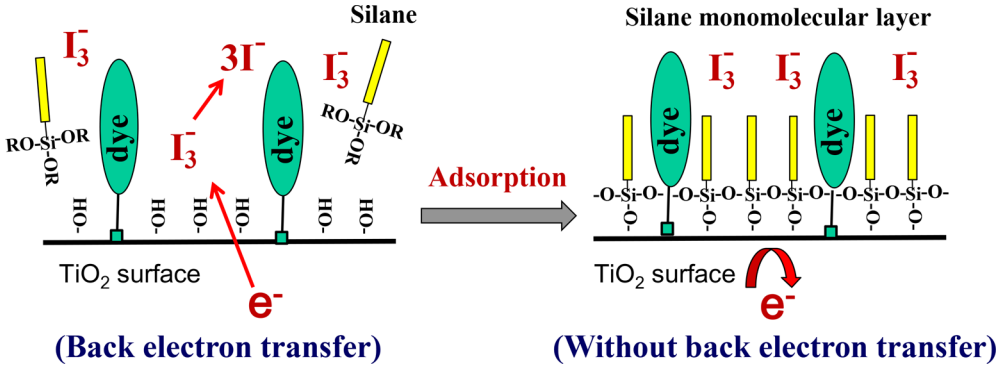

Figure 6. Schematic representation of self-assembled silane monomolecular layer formation on TiO_2 surface and blocking the back electron transfer.

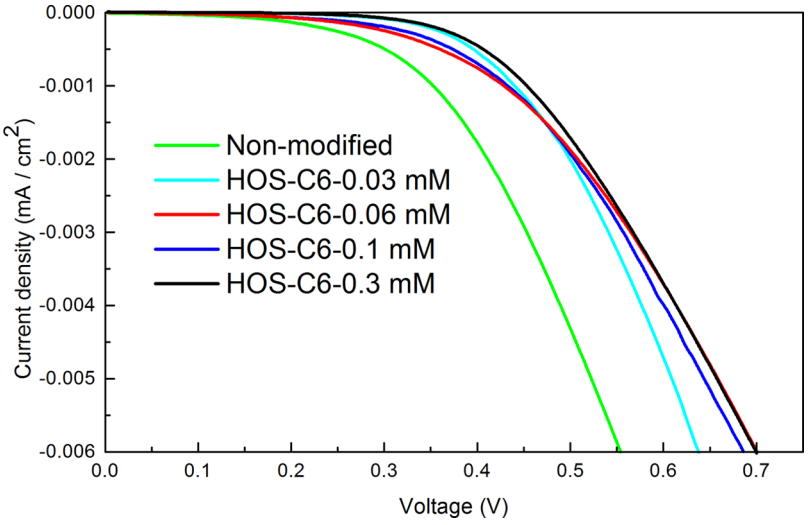

Figure 7. Dark $I-V$ characteristics of DSSCs fabricated using TiO_2 electrodes treated with different HOS-C6 concentrations.

However, the studies on the sequential adsorption of silane and dye have not yet been reported.

To improve J_{sc} by controlling the amount of silane and dye adsorbed, five types of treatment- process sequences were employed as follows: (1) dyeing without silanizing (dye), (2) dyeing followed by silanizing (dye/HOS), (3) silanizing followed by dyeing (HOS/dye), (4) simultaneous dyeing and silanizing (HOS+dye), and (5) dying followed by simultaneous dyeing and silanizing (dye/(HOS+dye)). HOS-C6 silane was used for silanizing. The effect of the treatment-process sequences on $I-V$ performances were investigated (see Figure S6 in the Supporting Information) and the results are summarized in Table 3. To more clearly examine the effect of a silane monolayer, we used a solution of 0.1 M LiI and 1.0 M I_2 in a mixed solvent of acetonitrile and valeronitrile (85%:15% volume ratio) as the electrolyte without any additives.

The cell parameters increase in order of (HOS+dye) < dye/HOS < HOS/dye < dye < dye/(HOS+dye) for J_{sc}, dye < HOS/dye < dye/(HOS+dye) < dye/HOS < (HOS+dye) for V_{oc}, (HOS+dye) < dye < HOS/dye < dye/(HOS+dye) < dye/HOS for FF, and (HOS+dye) < dye < HOS/dye < dye/HOS = dye/(HOS+dye) for η, respectively. These variations in $I-V$ characteristics could be attributed to the variation in surface coverage by dye and silane as described in the previous section.

Furthermore, EIS analyses were performed to understand the effects of these processes on the back electron transfer at interfaces. Estimated interfacial resistances and electron lifetime

Table 3. $I-V$ Characteristics and EIS (Electrochemical Impedance Spectroscopic) Characteristics of DSSCs Fabricated Using Different Silanizing and Dyeing Treatment Sequences

process	J_{sc} (mA/cm^2)	V_{oc} (V)	FF (%)	η (%)	R_s (Ω)	R_{Pt}(Ω)	R_{rc} (Ω)	τ (s)
dye	15.9	0.383	30	1.8	8	3	28	0.18
dye/HOS	12.2	0.444	47	2.6	6	3	100	0.36
HOS/dye	14.4	0.414	34	2.0	9	3	50	0.20
(HOS +dye)	11.6	0.453	29	1.5	5	3	79	0.63
dye/ (HOS +dye)	16.5	0.442	36	2.6	7	3	140	0.71

in TiO_2 electrode were made using impedance spectra (see Figure S7 in the Supporting Information) and are summarized in Table 3. The electron lifetime (τ) can be calculated using following formula

$$\tau = R_{rc}C_{\mu} = 1/\omega_{rec} \quad (3)$$

where R_{rc} is the interfacial resistance on TiO_2/electrolyte interface, C_{μ} is the chemical capacitance, and the ω_{rec} is the angular frequency.

Electron-transfer resistance from the working electrode to the counter electrode (R_s) and electron-transfer resistance from the counter Pt-electrode to the electrolyte solution (R_{pt}) have

dx.doi.org/10.1021/am500666e | ACS Appl. Mater. Interfaces 2014, 6, 5818−5826

not significantly been affected by silanization. But the interfacial resistance between electrons in the TiO_2 surface and the I_3^- in the electrolyte (R_{rc}) has been effectively improved in the every silanization process. The determined electron lifetimes are also in good agreement with the enhancements of the interfacial resistances. Although the other three processes impaired the J_{sc}, the dye/(HOS+dye) process improved J_{sc} slightly by 3.8% compared with the process without silanization. The dye/(HOS+dye) process also enhanced the V_{oc}, FF, and η by 15, 20, and 44%, respectively, and it is suggested to be the best process sequence. From this result, we found that photovoltaic performances can be optimized by varying the dyeing and silanizing process sequence.

3.4. DSSC Performance Modified with Different Type of Silanes. To investigate the effect of the different alkyl-chain length and substitutes on photovoltaic performance, we prepared DSSCs with TiO_2 electrodes, silanized using four different modifiers, HOS-C6, HOS-C10, HOS-C18, and FOS-C10F17. In this section, silane modifications were performed using optimum conditions of dye/(HOS+dye), as described in the previous section, and the electrolyte solution of 0.6 M butylmethylimidazolium iodide, 0.01 M I_2, 0.1 M LiI, 0.1 M guanidinium thiocyanate, and 0.4 M 4-tert- butylpyridine in a mixed solvent of acetonitrile and valeronitrile was used in the DSSC fabrication.

Figure 8 shows the $I-V$ characteristic curves of the DSSCs and Table 4 summarize the characteristic parameters. When

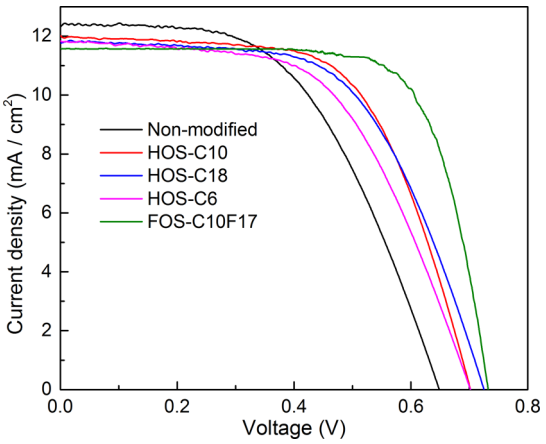

Figure 8. $I-V$ characteristics of DSSCs fabricated using TiO_2 electrodes treated with different kinds of silane solutions.

compared with unsilanized cell, every treated cell improved the V_{oc}, FF, and η of the DSSCs regardless of the silane structures. A small reduction of J_{sc} can be observed after silanization. It is very difficult to form the monolayer of silane only on the dye-uncovered TiO_2 surface.[3] The adsorption of silane molecules onto the dye molecules also may occur by a physical adsorption. Photoinduced adsorption spectroscopic studies have reported that the reduction of J_{sc} after several cycles of silanization is a result of a reduction of the dye regeneration rate.[12] They suggested that the silane molecules being adsorbed on the dye molecules could inhibit the dye regeneration reaction. In the present study we found that 37% of desorption of the dye after HOS-C6 silanization resulted corresponds to 36% of J_{sc} reduction. It suggested that the main reason for the reduction of J_{sc} after silanization is due to the dye desorption. We think that the silane with long-alkyl chain, such as HOS-C18, could give a steric hindrance on the oxidized dye regeneration reaction by I^-, but the effect would be small. However, silanization treatment substantially reduces the back electron transfer on the TiO_2 surface, which leads to high efficiency.

Interfacial resistance and electron lifetime were determined using impedance spectra (Figure 9) to clarify $I-V$ character-

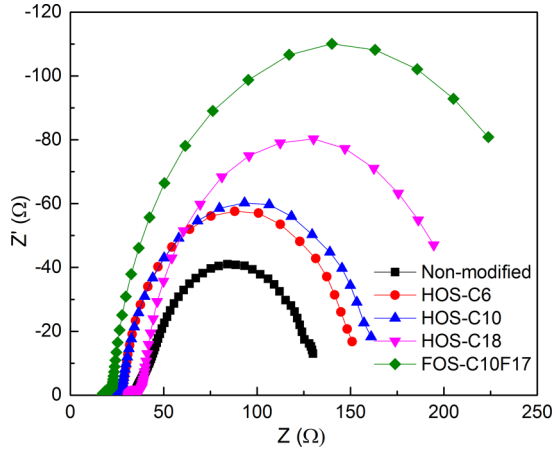

Figure 9. Impedance spectra of DSSCs prepared using dyeing followed by simultaneous dyeing and silanizing in different kinds of silane solutions.

istics. The interfacial resistances (R_{rc}) and the electron lifetimes (τ) derived from impedance spectra are summarized in Table 4. The R_{rc} and τ increase in the order of nonmodified < HOS-C6 < HOS-C10 < HOS-C18 < FOS-C10F17, which is nearly consistent with the variation in the V_{oc} and FF values. The results indicate that the V_{oc} and FF are improved due to the improvement in the R_{rc} and τ, which is a result of silanization. Increasing the alkyl-chain length of hydrocarbon silanes the R_{rc} and τ increase and a similar trend is observed with the TiO_2 electrodes without dyeing (Table 2). Although HOS-C18 showed the maximum V_{oc}, the maximum efficiency is given with HOS-C10 due to its comparatively high J_{sc} and FF values. We think that the main reason for the enhanced V_{oc} and FF are the suppression of the back electron transfer (loss of photoelectron from the TiO_2 surface with electrolyte) by the silane interposed layer. It has been reported that the suppression of the back electron transfer increases V_{oc} and FF.[6,8,14,28,29]

Among the four modifiers, FOS-C10F17 gives the optimum V_{oc} (0.735 V), FF (73.4%) and efficiency (6.2%) that enhances the efficiency by 48% compared with unsilanized cell. These results are also in good agreement with the largest R_{rc} and τ values, and the highest surface coverage and lowest K_{ad} obtained from adsorption isotherms (Table 2). It was found

Table 4. $I-V$ Characteristics and EIS (Electrochemical Impedance Spectroscopic) Characteristics of DSSCs Fabricated Using Different Silane Modifiers

sample	J_{sc} (mA/cm²)	V_{oc}(v)	FF (%)	η (%)	R_{rc} (Ω)	τ (s)
nonmodified	12.3	0.648	52.7	4.20	100	0.10
HOS-C6	11.8	0.700	56.6	4.68	125	0.16
HOS-C10	12.0	0.700	61.5	5.17	140	0.20
HOS-C18	11.7	0.730	59.2	5.06	200	0.50
FOS-C10F17	11.5	0.735	73.4	6.20	310	0.63

dx.doi.org/10.1021/am500666e | ACS Appl. Mater. Interfaces 2014, 6, 5818−5826

that high surface coverage and low K_{ad} are promising conditions to form an interposed layer without damaging or removing adsorbed dye molecules.

It has been reported that except the effect of the blocking back electron transfer, the surface functionalization of the TiO_2 electrode with coadsobants can shift the TiO_2 conduction band edge, which also affects V_{oc}.[6,14] The collective effect of a downward shift (toward positive potentials) of the band edges of TiO_2 by about 100 mV and slower the rate of back electron transfer by a factor of 20-fold results to a net improvement in V_{oc} of about 20 mV has been reported with a guanidinium adsorption.[9] Chenodeoxycholate coadsobant not only shifts the TiO_2 band edge to negative potentials (upward shift) by about 80 mV but also accelerates the rate of back electron transfer by a factor of 5-fold, which results to a net improvement in V_{oc} of over 40 mV.[30] The organic silanes have a high potential to suppress back electron transfer than decylphosphonic acid, undecanoic acid, and hemin, and a 7−330-fold decrease in the rate of back electron transfer can be achieved with the silane modifications.[14] Therefore, the V_{oc} enhancement in the present study could be ascribed mainly due to the suppression of back electron transfer by the silane adsorptions.

To fabricate a high-performance DSSC, we silanized an optimized TiO_2 electrode with scattering layer using FOS-C10F17 and the optimum conditions, TiO_2 film thickness of about 14 μm, silane treatment time of 2h, silane concentration of 0.06 mM, and silanization process sequence of (dye/(HOS +dye), which were found in this study were employed. The $I-V$ curves of DSSCs with silanization and without silanization are shown in Figure 10. Although the J_{sc} slightly decreases from

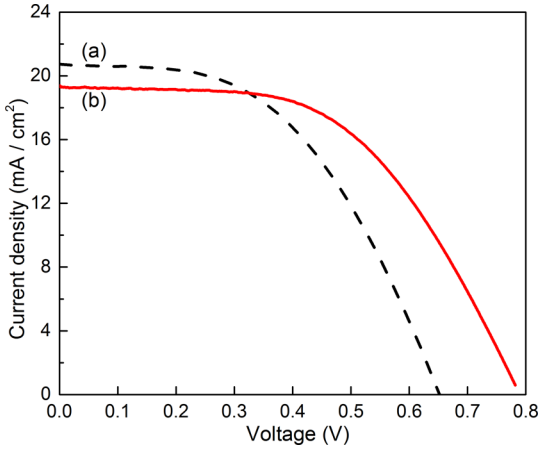

Figure 10. $I-V$ characteristics of DSSCs fabricated using optimized TiO_2 electrodes (a) without silanization and (b) with FOS-C10F17 silanization.

21.0 to 18.7 mA/cm^2, V_{oc} and FF are greatly improved from 0.65 V and 50% to 0.79 V and 54%, respectively, after silanization. Compared with DSSC without silanization (6.7%), DSSC with silanization (8.2%) showed 22% η enhancement. The result of this study also suggests that the {010}-faceted anatase TiO_2 nanoparticles, together with the FOS-C10F17 silane surface modification technique, are promising for the fabrication of the high performance DSSCs.

4. CONCLUSION

Silane adsorption on the surface of TiO_2 is dependent on the alkyl-chain length and substitutes of the silane. The Q_m, K_{ad}, and maximum surface coverage on TiO_2 surface decrease with increasing alkyl-chain length of hydrocarbon silanes. FOS-C10F17 fluorocarbon silane gives the highest surface coverage of the silanes included in this study. The silane adsorption can enhance the R_{rc} and τ of the TiO_2 electrode, which leads to improved values for V_{oc} and FF of DSSC. This effect increases with increasing alkyl-chain length of hydrocarbon silanes, and FOS-C10F17 shows the highest effect. The silanizing causes the dye desorption from the TiO_2 electrode, while the dye desorption can be suppressed by using the mixed solution of silane and dye in the silanizing process. The high performance DSSC is achieved using optimized silanizing conditions of FOS-C10F17, which yields a 22% improvement in efficiency, η.

■ ASSOCIATED CONTENT

Ⓢ Supporting Information

TG-DTA curves of HOS-C6 adsorbed TiO_2, variation of intensity ratio of Si−O/Ti−O vibration band with adsorption time, Nyquist plots of silanized TiO_2 electrodes, equivalent circuit diagram and model used to fit the impedance data, TG-DTA curves of HOS-C6 silanized and dyed TiO_2 nanoparticles, $I-V$ characteristics of DSSCs fabricated using TiO_2 electrodes treated by different treatment sequences, and impedance spectra of the DSSCs fabricated using TiO_2 electrodes modified with different treatment-process sequences. This material is available free of charge via the Internet at http://pubs.acs.org.

■ AUTHOR INFORMATION

Corresponding Author

*E-mail: feng@eng.kagawa-u.ac.jp.

Author Contributions

‡The manuscript was written through contributions of all authors. All authors have given approval to the final version of the manuscript. These authors contributed equally.

Notes

The authors declare no competing financial interest.

■ ACKNOWLEDGMENTS

This work was supported in part by Grants-in-Aid for Scientific Research (B) (23350101) from Japan Society for the Promotion of Science and Adaptable and Seamless Technology Transfer Program (AS242Z00679L) from Japan Science and Technology Agency.

■ REFERENCES

(1) O'Regan, B.; Grätzel, M. A Low-Cost, High-Efficiency Solar Cell based on Dye-Sensitized Colloidal TiO_2 Films. *Nature* **1991**, *353*, 737−740.

(2) Hara, K.; Arakawa, H. In *Handbook of Photovoltaic Science and Engineering*; Luque, A., Hegedus, S., Eds.; Wiley: Chichester, U.K., 2003; pp 670−671.

(3) Gregg, B. A.; Pichot, F.; Ferrere, S.; Fields, C. L. Interfacial Recombination Processes in Dye-Sensitized Solar Cells and Methods to Passivate the Interfaces. *J. Phys. Chem. B* **2001**, *105*, 1422−1429.

(4) Hagfeldt, A.; Grätzel, M. Molecular Photovoltaics. *Acc. Chem. Res.* **2000**, *33*, 269−277.

(5) Wen, P.; Xue, M.; Ishikawa, Y.; Itoh, H.; Feng, Q. Relationships between Cell Parameters of Dye-Sensitized Solar Cells and Dye-Adsorption Parameters. *ACS Appl. Mater. Interfaces* **2012**, *4*, 1928−1932.

(6) Huang, S. Y.; Schlichthörl, G.; Nozik, A. J.; Grätzel, M.; Frank, A. J. Charge Recombination in Dye-Sensitized Nanocrystalline TiO_2 Solar Cells. *J. Phys. Chem. B* **1997**, *101*, 2576−2582.

(7) Zhang, C.; Huang, Y.; Huo, Z.; Chen, S.; Dai, S. Photoelectrochemical Effects of Guanidinium Thiocyanate on Dye-Sensitized Solar Cell Performance and Stability. *J. Phys. Chem. C* **2009**, *113*, 21779−21783.
(8) Kay, A.; Grätzel, M. Artificial Photosynthesis. 1. Photosensitization of TiO_2 Solar Cells with Chlorophyll Derivatives and Related Natural Porphyrins. *J. Phys. Chem.* **1993**, *97*, 6272−6277.
(9) Kopidakis, N.; Neale, N. R.; Frank, A. J. Effect of an Adsorbent on Recombination and Band-Edge Movement in Dye-Sensitized TiO_2 Solar Cells: Evidence for Surface Passivation. *J. Phys. Chem. B* **2006**, *110*, 12485−12489.
(10) Ito, S.; Liska, P.; Comte, P.; Charvet, R.; Pechy, P.; Bach, U.; Mende, L. S.; Zakeeruddin, S. M.; Kay, A.; Nazeeruddin, M. K.; Grätzel, M. Control of Dark Current Photoelectrochemical (TiO_2/I^-−I_3^-) and Dye-Sensitized Solar Cells. *Chem. Commun.* **2005**, *34*, 4351−4353.
(11) Patrocínio, A. O. T.; Paterno, L. G.; Iha, N. Y. M. Layer-by-Layer TiO_2 Films as Efficient Blocking Layers in Dye-Sensitized Solar Cells. *J. Photochem. Photobiol., A* **2009**, *205*, 23−27.
(12) Feldt, S. M.; Cappel, U. B.; Johansson, E. M. J.; Boschloo, G.; Hagfeldt, A. Characterization of Surface Passivation by Poly(methylsiloxane) for Dye-Sensitized Solar Cells Employing the Ferrocene Redox Couple. *J. Phys. Chem. C* **2010**, *114*, 10551−10558.
(13) Spivack, J.; Siclovan, O.; Gasaway, S.; Williams, E.; Yakimov, A.; Gui, J. Improved Efficiency of Dye Sensitized Solar Cells by Treatment of the Dyed Titania Electrode with Alkyl(trialkoxy)silanes. *Sol. Energy Mater. Sol. Cells* **2006**, *90*, 1296−1307.
(14) Morris, A. J.; Meyer, G. J. TiO_2 Surface Functionalization to Control the Density of States. *J. Phys. Chem. C* **2008**, *112*, 18224−18231.
(15) García-González, C. A.; Saurina, J.; Ayllón, J. A.; Domingo, C. Preparation and Characterization of Surface Silanized TiO_2 Nanoparticles under Compressed CO_2: Reaction Kinetics. *J. Phys. Chem. C* **2009**, *113* (31), 13780−13786.
(16) Wen, P.; Ishikawa, Y.; Itoh, H.; Feng, Q. Topotactic Transformation Reaction from Layered Titanate Nanosheets into Anatase Nanocrystals. *J. Phys. Chem. C* **2009**, *113*, 20275−20280.
(17) Bernardoni, F.; Kouba, M.; Fadeev, A. Effect of Curvature on the Packing and Ordering of Organosilane Monolayers Supported on Solids. *Chem. Mater.* **2008**, *20*, 382−387.
(18) Helmy, R.; Fadeev, A. Y. Self-Assembled Monolayers Supported on TiO_2: Comparison of $C_{18}H_{37}SiX_3$ (X = H, Cl, OCH3), $C_{18}H_{37}Si(CH_3)_2Cl$, and $C_{18}H_{37}PO(OH)_2$. *Langmuir* **2002**, *18*, 8924−8928.
(19) Chen, Q.; Yakovlev, N. L. Adsorption and Interaction of Organosilanes on TiO_2 Nanoparticles. *Appl. Surf. Sci.* **2010**, *257*, 1395−1400.
(20) Shimizu, K.; Abel, M.-L.; Watts, J. F. Evaluation of the Interaction and Adsorption of Gamma-Glycidoxy propyl trimethoxysilane with Grit-Blasted Aluminium: A ToF-SIMS and XPS study. *J. Adhes.* **2008**, *84* (8), 725−741.
(21) Drummond, C. J.; Georgaklis, G.; Chan, D. Y. C. Fluorocarbons: Surface Free Energies and van der Waals Interaction. *Langmuir* **1996**, *12*, 2617−2621.
(22) Wang, Q.; Moser, J.-F.; Grätzel, M. Electrochemical Impedance Spectroscopic Analysis of Dye-Sensitized Solar Cells. *J. Phys. Chem. B* **2005**, *109*, 14945−14953.
(23) Fabregat-Santiago, F.; Garcia-Belmonte, G.; Mora-Sero, I.; Bisquert, J. Characterization of Nanostructured Hybrid and Organic Solar Cells by Impedance Spectroscopy. *Phys. Chem. Chem. Phys.* **2011**, *13*, 9083.
(24) Clifford, J. N.; Palomares, E.; Nazeeruddin, M. K.; Grätzel, M.; Durrant, J. R. Dye Dependent Regeneration Dynamics in Dye Sensitized Nanocrystalline Solar Cells: Evidence for the Formation of a Ruthenium Bipyridyl Cation/Iodide Intermediate. *J. Phys. Chem. C* **2007**, *111*, 6561−6567.
(25) Yum, J.-H.; Jang, S.-R.; Walter, P.; Geiger, T.; Nüesch, F.; Kim, S.; Ko, J.; Grätzel, M.; Nazeeruddin, M. K. Efficient Co-Sensitization of Nanocrystalline TiO_2 Films by Organic Sensitizers. *Chem. Commun.* **2007**, 4680−4682.
(26) Fan, S.-Q.; Kim, C.; Fang, B. Z.; Liao, K.-X.; Yang, G.-J.; Li, C.-J.; Kim, J.-J.; Ko, J. Improved Efficiency of Over 10% in Dye-Sensitized Solar Cells with a Ruthenium Complex and an Organic Dye Heterogeneously Positioning on a Single TiO_2 Electrode. *J. Phys. Chem. C* **2011**, *115*, 7747−7754.
(27) Shi, Y.; Liang, M.; Wang, L.; Han, H.; You, L.; Sun, Z.; Xue, S. New Ruthenium Sensitizers Featuring Bulky Ancillary Ligands Combined with a Dual Functioned Coadsorbent for High Efficiency Dye-Sensitized Solar Cells. *ACS Appl. Mater. Interfaces* **2013**, *5*, 144−153.
(28) Zhao, N.; Osedach, T. P.; Chang, L. Y.; Geyer, S. M.; Wanger, D. D.; Binda, M. T.; Arango, A. C.; Bawendi, M. G.; Bulovic, V. Colloidal PbS Quantum Dot Solar Cells with High Fill Factor. *ACS Nano* **2010**, *4*, 3743−3752.
(29) Usami, A. Theoretical Simulations of Optical Confinement in Dye-Sensitized Nanocrystalline Solar Cells. *Sol. Energy Mater. Sol. Cells* **2000**, *64*, 73−83.
(30) Neale, N. R.; Kopidakis, N.; van de Lagemaat, J.; Grätzel, M.; Frank, A. Effect of a Coadsorbent on the Performance of Dye-Sensitized TiO_2 Solar Cells: Shielding versus Band-Edge Movement. *J. Phys. Chem. B* **2005**, *109*, 23183−23189.